Preprints of the 18th IFAC World Congress
Milano (Italy) August 28 - September 2, 2011

Smooth Parametric Hysteresis Operator for Control

A. Katalenic * **C.M.M. van Lierop** * **P.P.J. van den Bosch** *

* *Department of Electrical Engineering, Eindhoven University of Technology, P.O. Box 513, 5600 MB Eindhoven, The Netherlands, E-mail: a.katalenic@tue.nl.*

Abstract: Hysteresis is a non-linear phenomenon present in many physical systems that is usually undesirable and degrades their performance. Models which accurately reproduce hysteresis are often very complex and hard to implement. For that reason, the hysteresis is generally, when the performance specifications are not too strict, treated as a bounded disturbance or is approximated with piecewise affine structures. Control design requires models which extract the most fundamental behavior of phenomena and, in this article, such a model was constructed for the hysteresis phenomenon. It is shown that the obtained model can be easily shaped, mathematically manipulated and used for general control design of hysteretic systems, e.g. feed-forward compensation.

Keywords: hysteresis; feedforward compensation; error analysis.

1. INTRODUCTION

Hysteresis is a phenomenon arising in many physical systems, such as electromagnetic actuators, mechanical transmissions, chemical processes, and financial markets. In the control society the word *hysteresis* generally refers to a persistent history dependant nontrivial closed curve in the input-output map of a system that does not collapse into a single-valued function for a quasi-static periodic inputs as discussed in Oh, Drincic, and Bernstein [2009]. This means that there is a certain *lag* between inputs and outputs of the system which is still present for infinitely slow periodic inputs. Linear systems, on the other hand, show no such behavior, meaning the hysteresis is inherently a nonlinear phenomenon. Throughout the literature in Oh, Drincic, and Bernstein [2009], Oh, and Bernstein [2005], Bertotti, and Mayergoyz [2006], hysteretic systems are generally split into *rate-dependant* and *rate-independent* hysteretic systems. The input-output map of the rate-dependent hysteretic systems changes with the frequency content of the input signal, meaning these systems are dynamical. On the other hand, systems with rate-independent hysteresis are completely described by their quasi-static behavior, thus making them effectively static. It is often argued as in Iyer, and Tan [2009], Su et al. [2000], Mittal, and Menq [2000] that the overall rate-dependent hysteretic behavior is due to some rate-independent hysteretic behavior present in the system coupled with non-hysteretic dynamical parts. Sometimes this separation is directly visible in the system architecture, as in the case of mechanical transmission, and sometimes this distinction is not very clear, as in the case of electromagnetic actuators with ferromagnetic cores. In this paper we follow the latter kind of approach, since it allows the separation of hysteretic and non-hysteretic parts of the system. Moreover, it allows for the usage of conventional control schemes together with the proposed hysteresis compensation techniques. The term *hysteresis* will be used to refer to the rate-independent hysteresis and the term *hysteretic system* will be used to refer to dynamical systems with hysteretic parts.

A large number of mathematical models of hysteresis have been developed in the following century of which the biggest number fall into the categories of integral models and Duhem models. Integral models of hysteresis include, among others, the popular Preisach model studied extensively in Bertotti, and Mayergoyz [2006] and the Prandtl-Ishilinskii model discussed in Su et. al [2009]. They are usually of high or infinite order and can be modified to accurately capture many phenomena present in ferromagnetic hysteresis. Their drawback is that they are hard to identify, are computationally complex and are usually not explicitly invertible, but regardless of that, due to fast digital processors, they are currently extensively used in control of systems with input hysteresis. On the other hand, the group of Duhem class models includes the Coleman-Hodgdon model discussed in Coleman, and Hodgdon [1986], and the Bouc-Wen model discussed in Ikhouane, Manosa, and Rodellar [2007] which are generally ordinary differential equations linking together input and output functions of time. Due to their elegant mathematical definition, these models are often used to model and study mathematical properties of hysteretic systems, but are not intended for direct implementation in control schemes because of the numerical problems and, sometimes, instability. Generally, it can be stated that the modeling of hysteresis was extensively studied in the past century, but there is a certain gap between modeling theory and control theory of hysteretic systems. Either a complex and accurate model is used to solve a specific problem as in Iyer, and Tan [2009], Mittal, and Menq [2000], Song, Zhao, and De Abreu-Garcia [2005], or

the hysteresis was treated as bounded disturbance as in Jayawardana, Logemann, and Ryan [2008], Su et al. [2000].

The main idea of this paper is to isolate the most fundamental behavior of the ferromagnetic and piezoelectric hysteresis into a simple, mathematically manipulable and implementable operator form. With having that in mind, a direct and inverse parametric hysteresis operator pair is constructed and it is shown that the simple behavior of these operators can further be extended to model more complex hysteresis without losing the basic structure and invertibility, meaning a general framework for modeling and analysis of hysteretic systems can be derived. In particular, this paper presents an approximative feed-forward hysteresis compensation scheme based on the parametric hysteresis operator together with a discussion of the compensation error bounds.

2. DIRECT AND INVERSE PARAMETRIC HYSTERESIS OPERATOR

We construct a scalar hysteresis operator with two modes which are described by smooth algebraic relations between the input and the output signal and which are shaped by two parameters. The analytical inverse and its derivatives are then constructed together with the error bounds due to parameter mismatch necessary for control design analysis. Its structure is motivated by the transition curves obtained when solving Duhem class hysteresis models for monotone inputs which are, in most cases, described by transcendental equations. For simple cases involving polynomials as exponential functions, the inverse of these functions can be explicitly expressed using the lambert w function. We use this fact, but reverse the order, and state that the transition curves of the direct hysteresis model are defined by the lambert w function, so the inverse is expressed using polynomials and exponential functions.

The following transformations define the switching instances and the initial values for the direct and the inverse hysteresis model which will be necessary to define the operator for general input signals:

Definition 2.1. Let $\alpha_0, \beta_0 \in \mathbb{R}$ and $\alpha(t), \beta(t) : \mathbb{R}^+ \to \mathbb{R}$ belong to class C^∞ and C^1 respectively. Define the transformation:

$$T(\alpha(t), \beta(t)) = \begin{cases} [\alpha(t) - \alpha_0, \beta(t) - \beta_0] & \text{for } \dot{\alpha}(t) \geq 0 \\ [\alpha_0 - \alpha(t), \beta_0 - \beta(t)] & \text{for } \dot{\alpha}(t) < 0 \end{cases}$$

and the function:

$$M(\alpha(t), \beta(t)) = \begin{cases} \beta_0 - \alpha_0 & \text{for } \dot{\alpha}(t) \geq 0 \\ -\beta_0 + \alpha_0 & \text{for } \dot{\alpha}(t) < 0, \end{cases}$$

where $\alpha_0 = \alpha(\tau^*)$ and $\beta_0 = \beta(\tau^*)$ with:

$$\tau^* = \begin{cases} \sup\limits_{\dot{\alpha}(\tau)=0, \ddot{\alpha}(\tau)\neq 0, \tau \leq t} \tau & \text{for } t > 0 \\ 0 & \text{for } t = 0, \end{cases}$$

i.e. τ^* is the last time instant at which $\dot{\alpha}(t)$ changed sign.

Basically, if $\alpha(t)$ and $\beta(t)$ are put in a Cartesian coordinate system, then α_0 and β_0 define values of $\alpha(t)$ and $\beta(t)$ in the last time instance when the input signal changes direction, $T(\alpha, \beta)$ defines the current position of $\alpha(t)$ and $\beta(t)$ relative to α_0 and β_0 and $M(\alpha, \beta)$ defines the vertical distance of that point to the $\beta(t) = \alpha(t)$ line. Furthermore,

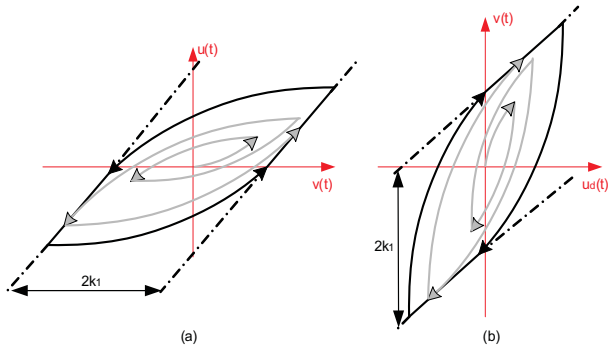

Fig. 1. Input-output map of the direct hysteresis operator (a) and the inverse hysteresis operator (b) with the periodic input of increasing amplitude.

these transformations have memory since they store values of α_0 and β_0.

Throughout the paper, a tilde notation over a symbol will be used to denote variables transformed as in definition 2.1, while a bar notation over a symbol will be used to denote estimated, non-exact values of parameters. Both notations require previous definitions of symbols they are used on.

Definition 2.2. Let $v(t), u(t) \in C^\infty$, $k_1, k_2, M \in \mathbb{R}^+$ and let W be the principal branch of the Lambert W function. Then the *direct parametric hysteresis operator* :

$$u(t) = H(k_1, k_2)[v(t)] \tag{1}$$

is defined as:

$$\tilde{u}(t) = \tilde{v}(t) - M^* + \frac{1}{k_2} W\left(k_2 M^* \cdot e^{k_2(M^* - \tilde{v}(t))}\right) \tag{2}$$

where $[\tilde{v}(t), \tilde{u}(t)] = T(v(t), u(t))$, $M^* = M(v(t), u(t)) + k_1$, $v(t)$ denotes the input to the operator and $u(t)$ denotes the output of the operator.

Remark 2.3. The model (2) is bounded by two affine asymptotes, that is, when $v(t) \to \infty \Longrightarrow H(v(t)) = v(t) - k_1$ and when $v(t) \to -\infty \Longrightarrow H(v(t)) = v(t) + k_1$. This is seen by substituting for M^* and using the fact that $W(0) = 0$. It means (1) is a *backlash-like* hysteresis operator. All other effects, such as the slope of the loop, are not considered as part of the hysteresis and are treated as part of the remaining system.

Remark 2.4. The parameter k_1 represents the "amount of hysteresis" around the line $v(t) = u(t)$ and defines the asymptotes , while the parameter k_2 represents the rate of the smooth transition towards these asymptotes as seen in Fig. 1 (a).

Definition 2.5. Let $v(t), u_d(t) \in C^\infty$, $k_1, k_2 \in \mathbb{R}^+$. Then the *inverse parametric hysteresis operator* :

$$v(t) = H^{-1}(k_1, k_2)[u_d(t)] \tag{3}$$

is defined as:

$$\tilde{v}(t) = \tilde{u}_d(t) + M^* \cdot \left(1 - e^{-k_2 \tilde{u}_d(t)}\right) \tag{4}$$

where $[\tilde{u}_d(t), \tilde{v}(t)] = T(u_d(t), v(t))$, $M^* = -M(u_d(t), v(t)) + k_1$, $u_d(t)$ denotes the input to the operator and $v(t)$ denotes the output of the operator.

The inverse hysteresis operator is also bounded by two affine asymptotes and is parameterized by k_1, which de-

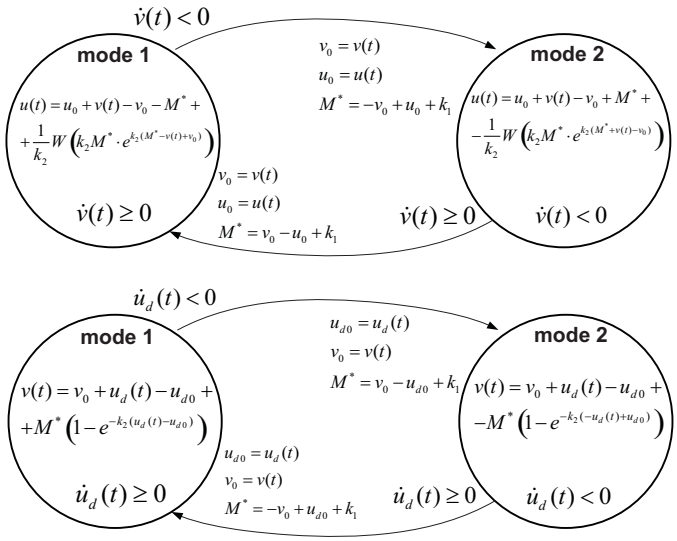

Fig. 2. Automata representation of the direct (2) and inverse (4) hysteresis operator.

fines the amount of hysteresis, and k_2 ,which defines the rate of transition towards the asymptotes as seen in Fig. 1.

Remark 2.6. Both direct (2) and inverse (4) hysteresis operators can operate in two modes. The automata representation of both operators is shown in Fig. 2.

Proposition 2.7. The first time derivative:

$$\dot{v}(t) = \dot{H}^{-1}(u_d(t), \dot{u}_d(t)) \tag{5}$$

and the second time derivative:

$$\ddot{v}(t) = \ddot{H}^{-1}(u_d(t), \dot{u}_d(t), \ddot{u}_d(t)) \tag{6}$$

of the inverse parametric hysteresis operator are given by:

$$\dot{v}(t) = \left(1 + k_2 M^* \cdot e^{-k_2 \tilde{u}_d(t)}\right) \dot{u}_d(t), \tag{7}$$

$$\ddot{v}(t) = \left(1 + k_2 M^* \cdot e^{-k_2 \tilde{u}_d(t)}\right) \ddot{u}_d(t) - M^* {k_2}^2 \cdot e^{-k_2 \tilde{u}_d(t)} \dot{u}_d^2, \tag{8}$$

where $[\tilde{u}_d(t), \tilde{v}(t)] = T\left(u_d(t), v(t)\right)$ *and* $M^* = M(u_d(t), v(t)) + k_1$.

These expressions are obtained by differentiating (4) and will be used for feed-forward controller synthesis. The implementation of these operators requires time derivatives of the input signal which can be made available in feed-forward compensation schemes as discussed in section 5. Because the transition functions in both modes are infinitely smooth and the values of the operators are uniquely defined at the switching instances through definition 2.1, i.e. with the left limit, time derivatives of the operators are also uniquely defined and bounded over the switching instances, e.g. if $u_d(t) \in C^1$ then $v(t) \in C^1$, $\dot{v}(t) \in C^0$ and $\ddot{v}(t), \dddot{v}(t), \ldots \in C^{-1}$, i.e. second and higher time derivatives are discontinuous, but bounded. Higher time derivatives can be constructed from (8) by further differentiation.

Definition 2.8. A *family of parametric hysteresis operators* is defined as:

$$RH(k_1, \Delta k_1, k_2, \Delta k_2) = \left\{H(k_1^*, k_2^*), |k_1 - k_1^*| \leq \Delta k_1, |k_2 - k_2^*| \leq \Delta k_2\right\} \tag{9}$$

A *family of inverse parametric hysteresis operators* is defined as:

$$RH^{-1}(k_1, \Delta k_1, k_2, \Delta k_2) = \left\{H^{-1}(k_1^*, k_2^*), |k_1 - k_1^*| \leq \Delta k_1, |k_2 - k_2^*| \leq \Delta k_2\right\} \tag{10}$$

A set of all possible trajectories generated by the given family RH is then: $\Upsilon(RH)\left[v(t)\right] = \{H[v(t)], H \in RH\}$.

Some random scalar rate-independent hysteresis $Hyst(\cdot)$ is said to be *reproducible by the family RH* in some working interval $L = [v_{min}, v_{max}]$ if:

$$Hyst(v(t)) \in \Upsilon(RH)\left[v(t)\right], \forall v(t) \in L,$$

i.e. if, at a given time instant, there exists a parametric hysteresis operator within the family that gives the same output for the given input $v(t)$.

In practice, a family of direct hysteresis operators will be used to model the hysteresis present in some system.

3. ERROR BOUNDS DUE TO PARAMETER MISMATCH

When using the exact hysteresis inverse to compensate for hysteresis described by a family of parametric hysteresis operators, a certain compensation error is induced. In this section we discuss guaranteed bounds on these errors.

The following inequalities, which simplify the error analysis, were found to be valid for the lambert W function:

Lemma 3.1. Let $a \in \mathbb{R}^+$,$b \in \mathbb{R}$ *and let* W *be the principal branch of the Lambert W function, then:*

$$W\left(a \cdot e^b\right) = a = b, \qquad \text{if} \quad a = b, \tag{11a}$$

$$a \leq W\left(a \cdot e^b\right) < b, \qquad \text{if} \quad a < b, \tag{11b}$$

$$b < W\left(a \cdot e^b\right) < a, \qquad \text{if} \quad a > b. \tag{11c}$$

Proof. Equality (11a) follows from the definition of the Lambert W function as in Corless et al. [1996]. To prove (11b) and (11c), let $W_a(a,b) = \frac{\partial W(a \cdot e^b)}{\partial a} = \frac{W(a \cdot e^b)}{a(1 + W(a \cdot e^b))}$, $W_{aa}(a,b) = \frac{\partial^2 W(a \cdot e^b)}{\partial a^2} = -\frac{W(a \cdot e^b)^2\left(2 + W(a \cdot e^b)\right)}{a^2(1 + W(a \cdot e^b))^3}$, $W_b(a,b) = \frac{\partial W(a \cdot e^b)}{\partial b} = \frac{W(a \cdot e^b)}{1 + W(a \cdot e^b)}$. It is easy to see that for $x \geq 0$ it follows that $W(x) \geq 0$ because $W(x)e^{W(x)} = x \geq 0$ and $e^{W(x)} \geq 0$. Then $\frac{dW(x)}{dx} = \frac{W(x)}{x(1 + W(x))} \geq 0$ for $x \geq 0$, meaning $W(x)$ is monotone w.r.t. x for $x \geq 0$. The value of $\frac{dW(x)}{dx}$ for $x = 0$ can be calculated by analyzing the Taylor expansion of $W(x)$ around $x = 0$: $W(x) = x - x^2 + \frac{3}{2}x^3 - \ldots$. From this we have $\frac{dW(x)}{dx} = 1 + x(\ldots)$, so $\frac{dW(x)}{dx}(x = 0) = 1$. Similarly it follows that $\frac{dW(a \cdot e^b)}{da}(a = 0) = e^b$. Then since $a \geq 0$, it also follows that $a \cdot e^b \geq 0$, and $W(a \cdot e^b) \geq 0$.

Observe that $W(a, b = a) = a$ and $W_{aa}(a \geq 0, b) \leq 0$, meaning $W(a \cdot e^b)$ is concave for any fixed $b \geq 0$. Then because $W_a(a, b = a) = \frac{1}{1+a} < 1$ it follows that $W\left(a \cdot e^b\right) < a$, for every $a > b \geq 0$. It is also valid for $a > 0, b < 0$, since e^b is monotone w.r.t. b and $W(x)$ is monotone w.r.t. x for $x \geq 0$, yielding: $W(a \cdot e^c) \leq W(a \cdot e^b)$, for c ≤ b.

Furthermore, because $\lim_{a \to 0} W_a(a,b) = e^b \geq 1$ for $b \geq 0$ and $W(a \cdot e^b)$ is concave for $a \geq 0$ and any fixed $b \geq 0$, it follows that $a \leq W(a \cdot e^b)$, for $a < b$.

Moreover, from $W(a=b,b)=b$ and $0 \leq W_b(a,b) \leq 1$, it follows that $W(a \cdot e^b) < b, \quad \text{for} \quad a < b$, and $b < W(a \cdot e^b), \quad \text{for} \quad a > b$. □

We find these inequalities applicable in the error analysis for many others problems where lambert w is used to construct the solution and when there is some uncertainty in the parameters.

Proposition 3.2. The maximum additive error of the output of the inverse hysteresis operator $H^{-1}(k_1,k_2)$ compared to the outputs of the whole family of inverse parametric hysteresis operators $RH^{-1}(k_1,\Delta k_1,k_2,\Delta k_2)$ is given by:

$$\begin{aligned} &\max\left|H^{-1}(\bar{k}_1,\bar{k}_2) - H^{-1}(k_1,k_2)\right| = \\ &= |\Delta_a| \leq \max(|\Delta_{x1}|,|\Delta_{x2}|,|\Delta_{x3}|,|\Delta_{x4}|), \end{aligned} \tag{12}$$

with $\bar{k}_1 \in [k_1-\Delta k_1, k_1+\Delta k_1]$ and $\bar{k}_2 \in [k_2-\Delta k_2, k_2+\Delta k_2]$ and $\Delta_{x1},\Delta_{x2},\Delta_{x3},\Delta_{x4}$ obtained by evaluating: $\Delta_x(k_1,\bar{k}_1,k_2,\bar{k}_2) = \bar{k}_1 - k_1 + 2(k_1 e^{-k_2 x} - \bar{k}_1 e^{-\bar{k}_2 x})$ and with $x = \max\left(\frac{\ln\frac{\bar{k}_1\bar{k}_2}{k_1 k_2}}{\bar{k}_2-k_2}, 0\right)$ in the four points of maximal parameter deviation:

$$\begin{aligned} \Delta_{x1} &= \Delta_x(k_1, k_1-\Delta k_1, k_2, k_2-\Delta k_2) \\ \Delta_{x2} &= \Delta_x(k_1, k_1-\Delta k_1, k_2, k_2+\Delta k_2) \\ \Delta_{x3} &= \Delta_x(k_1, k_1+\Delta k_1, k_2, k_2-\Delta k_2) \\ \Delta_{x4} &= \Delta_x(k_1, k_1+\Delta k_1, k_2, k_2+\Delta k_2) \end{aligned} \tag{13}$$

Also, for sufficiently large $\tilde{u}_d(t)$, the additive error converges to the interval: $|\Delta_a| \leq \Delta k_1$.

Proof. We calculate the error: $\Delta_a = \bar{v}(t) - v(t) = H^{-1}(\bar{k}_1,\bar{k}_2)[u_d(t)] - H^{-1}(k_1,k_2)[u_d(t)]$ by inserting (4) and get: $\Delta_a(\tilde{u}_d(t)) = \bar{k}_1 - k_1 + (M^* e^{-k_2 * \tilde{u}_d(t)} - \bar{M}^* e^{-\bar{k}_2 \tilde{u}_d(t)})$. Using the fact that the width of the hysteresis loop is bounded by $2k_1$, it follows that $M^* \leq 2k_1$ and we obtain:

$$|\Delta_a(\tilde{u}_d)| \leq |{\Delta_x}^*(\tilde{u}_d)| = |\bar{k}_1 - k_1 + 2(k_1 e^{-k_2\tilde{u}_d} - \bar{k}_1 e^{-\bar{k}_2\tilde{u}_d})|. \tag{14}$$

The extremum point x is the point where $\frac{\partial {\Delta_x}^*}{\partial \tilde{u}_d} = 0$, i.e. the extremum point of ${\Delta_x}^*$. Since (14) is defined for negative arguments as well, they have to be ruled out because $\tilde{u}_d(t) \geq 0$. Further since $\frac{\partial {\Delta_x}^*}{\partial \bar{k}1} < 0$ and $\frac{\partial {\Delta_x}^*}{\partial \bar{k}_2} \geq 0, \ \forall \ \tilde{u}_d, k_1, \bar{k}_1, k_2, \bar{k}_2 \geq 0$, it follows that the bounds on the error values inside the given interval are defined by the values of the error at the end-points. All four end-points in (13) have to be checked since the values of ${\Delta_x}^*$ inside the interval pass through zero. The biggest value of the error function at these points defines the final bound. □

Proposition 3.3. The bound on the maximal error of the output of the family of parametric hysteresis operators $RH(k_1,\Delta k_1,k_2,\Delta k_2)$ compared to the signal $u_d(t)$ when the input to the family equals $v(t) = H^{-1}(k_1,k_2)[u_d(t)]$ is given by:

$$|\Delta_b| \leq |\Delta_a| \tag{15}$$

where Δ_a is the error bound discussed in proposition 3.2, and $\Delta_b = H(\bar{k}_1,\bar{k}_2)[H^{-1}(k_1,k_2)[u_d(t)]] - u_d(t)$.

Proof. Observe that $\frac{\partial u(v(t))}{\partial v(t)} = 1 - \frac{W(k_2 M^* e^{k_2(M^*-\bar{v}(t))})}{1+W(k_2 M^* e^{k_2(M^*-\bar{v}(t))})}$, where $u(v(t)) = H[v(t)]$. Because $W\left(k_2 M^* e^{k2(M^*-\tilde{v}(t))}\right) \geq 0$, $\forall \tilde{v}(t)$ it follows that $0 \leq \frac{\partial u(v(t))}{\partial v(t)} \leq 1$, $\forall \tilde{v}(t)$, i.e. the tangent on the input-output map of the direct hysteresis operator is always in the interval between zero and one. That implies: $|H[v(t)+\Delta_a] - H[v(t)]| = \left|\int_{v(t)}^{v(t)+\Delta_a} \frac{\partial H[\vartheta]}{\partial \vartheta} d\vartheta\right| \leq |\Delta_a|$. The input to the family of direct hysteresis operators can be written as $v(t) = H^{-1}(k_1,k_2)[u_d(t)] = H^{-1}(\bar{k}_1,\bar{k}_2)[u_{\bar{d}}(t)] + \Delta_a$. Then we get: $|\Delta_b| = |H(\bar{k}_1,\bar{k}_2)[H^{-1}(\bar{k}_1,\bar{k}_2)[u_d(t)]+\Delta_a] - u_d(t)| \leq |\Delta_a|$, that is: $|\Delta_b| \leq |\Delta_a|$. □

4. PROPERTIES OF THE PARAMETRIC HYSTERESIS OPERATOR

4.1 Initial conditions and invertibility

Proposition 4.1. The inverse parametric hysteresis operator (3) is the exact left and right analytical inverse of the direct hysteresis operator (1) when the operator parameters k_1 and k_2 and the initial conditions, $u_{d0}(t=0)$ and $u_0(t=0)$, are the same.

Proof. Inputting (4) with $\bar{M}^* = M^*$ into (2) yields:

$$\begin{aligned} \tilde{u}(t) &= \tilde{u}_d(t) + \bar{M}^* - \bar{M}^* e^{-k_2\tilde{u}_d(t)} - M^* + \\ &+ \frac{1}{k_2} W\left(k_2 M^* \cdot e^{k_2(M^*-\bar{M}^*)} e^{-k_2\tilde{u}_d(t)} e^{k_2\bar{M}^* e^{-k_2\tilde{u}_d(t)}}\right). \end{aligned} \tag{16}$$

Due to the monotonicity property of both the direct and the inverse hysteresis operators, it holds that $sign(\dot{u}_d(t)) = sign(\dot{v}(t)) = sign(\dot{u}(t))$ and assuming the same initial conditions, i.e. $u_{d0}(t=0) = u_0(t=0) \Rightarrow u_{d0} = u_0$, we get: $M^* - \bar{M}^* = u_0 - v_0 + k_1 - u_{d0} + v_0 - k_1 = 0 \Rightarrow M^* = \bar{M}^*$. Then (16) becomes: $\tilde{u}(t) = \tilde{u}_d(t) - \bar{M}^* e^{-k_2\tilde{u}_d(t)} + \frac{1}{k_2} W\left(k_2 M^* \cdot e^{-k_2\tilde{u}_d(t)} e^{k_2\bar{M}^* e^{-k_2\tilde{u}_d(t)}}\right)$. By applying lemma 3.1, we get: $\tilde{u}(t) = \tilde{u}_d(t)$, which with $u_{d0} = u_0$ gives: $u(t) = u_d(t)$. Proving that (3) is also the right inverse of (1) is done in a similar way by using the equality $x = W(x)e^{W(x)}$ discussed in Corless et al. [1996]. □

Proposition 4.2. If the initial conditions in proposition 4.1 are not the same, i.e. $u_{d0}(t=0) \neq u_0(t=0) \Rightarrow M^*(t=0) \neq \bar{M}^*(t=0)$, then the error $u(t) - u_d(t)$ will converge asymptotically towards zero under the condition that $\lim_{t\to\infty} \dot{u}_d(t) \neq 0$, i.e. the excitation is persistent, e.g. a periodic or a ramp signal.

Proof. Using lemma 3.1 on (16) with a substitution $\Delta = \bar{M}^* - M^*$ gives: $\tilde{u}(t) \in \tilde{u}_d(t) + \Delta - \bar{M}^* e^{-k_2\tilde{u}_d(t)} + \left[M^* e^{-k_2\Delta}, \bar{M}^*\right] e^{-k_2\tilde{u}_d(t)}$, where $[-,-]$ denotes a closed interval. Since v_0 must be the same in both operators, using the transformations defined in 2.2 and 2.5 it follows that $\tilde{u}(t) - \tilde{u}_d(t) = u(t) - u_d(t) + \Delta$. Then:

$$u(t) - u_d(t) \in \left[M^* e^{-k_2\Delta} - \bar{M}^*, 0\right] e^{-k_2\tilde{u}_d(t)}. \tag{17}$$

If $u(\tau^*) - u_d(\tau^*) \geq 0$ then $M^* \geq \bar{M}^*$ meaning $\Delta \leq 0$ and, with (17), that $u(t) - u_d(t)$ equals some positive value from the interval which is exponentially decaying with $\tilde{u}_d > 0$. Also, if $u(\tau^*) - u_d(\tau^*) < 0$ then $M^* < \bar{M}^* \to \Delta > 0$ and $u(t) - u_d(t)$ equals some negative values from the interval which also converges exponentially towards 0 for $\tilde{u}_d(t) > 0$.

If $t = \tau_2^*$ is the next moment of input signal direction change, then new $u_0 = u(\tau_2^*)$ and $u_{d0} = u_d(\tau_2^*)$ are defined together with new M_2^* and $\bar{M}_2^*$ and $|\Delta_2| = |\bar{M}_2^* - M_2^*| = |u_d(\tau_2^*) - u(\tau_2^*)| < |u_d(\tau^*) - u(\tau_2^*)| = |\Delta|$ since $|u(t) - u_d(t)|$ decays exponentially. □

4.2 Causality, monotonicity, passivity and accommodation

Causality: The transformations from the definition 2.1 which are used to construct the hysteresis operator pair require knowledge of the time derivative of the input signal. When implementing these transformations on a digital computer, they can be made causal by assuming: $\dot{v}(t) = \frac{v(k)-v(k-1)}{T}$. This generates no significant error since only $sign(\dot{v}(t))$ is needed.

Monotonicity: Differentiating (4) yields $\dot{v}(t) = \dot{u}_d(t) + M^* k_2 e^{k_2 \tilde{u}_d(t)} \dot{u}_d(t)$. For $\dot{u}_d(t) \geq 0$ we get $\tilde{u}_d(t) \geq 0$ yielding $\dot{v}(t) \geq 0$. Similarly, it can be shown that $\dot{u}_d(t) \leq 0$. Also, the monotonicity of the inverse hysteresis operator directly implies the monotonicity of the direct hysteresis operator.

Passivity: Analyzing (2) with $k_1, k_2 > 0$ for ascending and descending input signals shows that if $\dot{v}(t) \geq 0$ then $u(t) \leq v(t)$ and if $\dot{v}(t) < 0$ then $u(t) > v(t)$. This means that only counter-clockwise curves can be closed in the input-output map of the operator, therefore showing the operator (1) is *passive*, D. Angeli [2006].

Accommodation: For periodic inputs, the operator (1) always forms limit cycles which are antisymmetric around the $u(t) = v(t)$ line. This can be demonstrated by observing what happens when an infinitely small periodic signal is applied to (3) with $u_{d0} \neq v_0$, i.e. when there is some initial offset from the $u(t) = v(t)$ curve. If $v_0 > u_{d0}$, M^* in case $\dot{u}_d(t) \geq 0$ will always be smaller then M^* in case $\dot{u}_d(t) < 0$. This can be seen from (4) where $M^* = -M(u_d(t), v(t)) + k_1$. Analyzing (4) for small inputs then gives : $\Delta\tilde{v} \approx (1 + k_2 M^*)\Delta\tilde{u}_d$. Since M^* is larger in case $\dot{u}_d(t) < 0$, it follows that $|\Delta\tilde{v}|$ is larger in case $\dot{u}_d(t) < 0$, meaning $\Delta\tilde{u}_d < 0$ and $v(t)$ decreases. The opposite can be obtained for $v_0 < u_{d0}$ showing that all trajectories will be attracted towards $v(t) = u_d(t)$ line, which is in fact the anhysteretic curve of the proposed model. Then the same must be true for (1). Accommodation to the anhysteretic curve is not a property observed in magnetic hysteresis and is thus a non-desired effect of the proposed operator.

4.3 Shaping the model

A smooth, monotone and invertible function ψ can be applied to the input or the output signal of the parametric hysteresis operator. It will be called a *shaping function* since it shapes the initially affine boundaries of the proposed hysteretic operator to match potentially curved boundaries of the measured hysteresis. A good examples of the shaping function is the *langevin function* $\psi(x) = \coth(x) - \frac{1}{x}$ which is often used as an approximation of the *anhysteretic curve* of magnetic materials and the hyperbolic tangent, i.e. $\psi(x) = \tanh(x)$. Using invertible shaping functions does not impair the invertibility of the operator, since they are outside the operator and can be treated as part of the remaining dynamical system.

Furthermore, in order to model more complex hysteresis, the transition smoothness parameter k_2 can be made a function of the input, i.e. $k_2 = \varphi(v(t))$. However, as a consequence, the inverse operator (3) is no longer the analytical inverse of (1), but can be approximated as discussed in the proposition that follows.

Proposition 4.3. The direct parametric hysteresis operator $H(k_1, \varphi(v(t)))[v(t)]$ can be approximately inverted in the working interval $L = [v_{min}, v_{max}]$ by the inverse operator $H^{-1}(k_1, \varphi(u_d(t)))[u_d(t)]$ where the maximal deviation of the parameter k_2 for sufficiently smooth φ is given by $\Delta k_2 \leq \sup_{v(t)\in L} \frac{d\varphi(v(t))}{dv(t)} k_1$. When maximal parameter deviations are known, the expressions (12) and (15) can be used to compute the compensation error bound.

Proof. From the definition of the inverse hysteresis operator and considering the remark 2.3, it follows that $|v(t) - u_d(t)| \leq k_1$. The "amount of hysteresis" k_1 can often be assumed small compared to the working interval L and when the function φ is sufficiently smooth, the approximation $\frac{\varphi(v(t))-\varphi(u_d(t))}{v(t)-u_d(t)} \approx \frac{d\varphi(v(t))}{dv(t)}$ can be used. If φ is affine in $v(t)$, this is an equality. The final maximal deviation is then obtained by finding the maximum over the interval L and by using the fact that $\Delta k_2 = \varphi(v(t)) - \varphi(u_d(t)$. □

5. FEED-FORWARD HYSTERESIS COMPENSATION

If the hysteresis is present at the system input, i.e. it is directly reachable by the controller, it can be directly compensated. In this case, the parameters of the direct hysteresis operator, together with the shaping functions obtained when modeling the system hysteresis, are directly used to construct the hysteresis inverse (3). When the input hysteresis is not reproducible with a single parametric hysteresis operator, a family of operators has to be used as discussed in definition 2.8. When the compensation is not exact, the maximal error bound of the compensation scheme is discussed in propositions 3.2 and 3.3. If the hysteresis is preceded by some dynamics, the following lemma applies:

Lemma 5.1. Consider a dynamical system with rate - independent hysteresis preceded by some stable linear dynamics:

$$\begin{aligned} &\frac{x_1(s)}{u(s)} = \frac{b}{a_n s^n + a_{n-1} s^{n-1} + \ldots + 1} \\ &x_2(t) = Hyst(x_1(t)) \\ &\ldots \end{aligned} \tag{18}$$

where $x_1(s) = \mathcal{L}\{x_1(t)\}$ and $Hyst(\cdot)$ is some rate-independent hysteresis that is reproducible by the robust parametric hysteresis family $RH(k_1, \Delta k_1, k_2, \Delta k_2)$. Then, after the transients due to initial conditions, the compensation law:

$$u(t) = \frac{1}{b}\left\{ a_n \frac{d^n}{dt^n} + a_{n-1} \frac{d^{n-1}}{dt^{n-1}} + \ldots + 1 \right\} H^{-1}[v(t)] \tag{19}$$

with $v^{(n)}(t) = u_{new}(t)$ renders the system into:

$$\begin{aligned} &x_2^{(n)} = u_{new}(t) + \Delta \\ &\ldots \end{aligned} \tag{20}$$

where $\frac{d^k}{dt^k}, k \in \{1, \ldots, n\}$ *is a differential operator acting on* H^{-1} *which is defined in proposition 2.7, and* $|\Delta| \leq |\Delta_a|$ *is the error bound (12). Also, when* $\Delta k_1, \Delta k_2 = 0$*, there is no compensation error, i.e.* $\Delta = 0$.

Proof. After inputting (19) into (18), the following linear differential equation is obtained:

$$\left\{a_n \frac{d^n}{dt^n} + \ldots + 1\right\} x_1(t) = \left\{a_n \frac{d^n}{dt^n} + \ldots + 1\right\} H^{-1}\left[v(t)\right] \tag{21}$$

A particular solution to the equation (21) is $x_1(t) = H^{-1}\left[v(t)\right]$. Because the dynamics (18) are stable, all the solutions to the related homogeneous equation of (21) will decay with time. If the initial conditions in the left hand and right hand side of (21) match, then the general solution is unique and the equality $x_1(t) = H^{-1}\left[v(t)\right]$ holds for every $t > 0$. Furthermore, in order to be able to construct time derivatives of H^{-1} in (19), time derivatives of $v(t)$ are required to be known, meaning the input of the compensator has to be integrated n times, i.e. $v(t) = \int \ldots \int u_{new}(t) dt \ldots dt$. This gives: $x_2(t) = Hyst\left(H^{-1}\left[v(t)\right]\right)$ which together with the results from the proposition 3.3 gives the final expression (20). The hysteresis and the preceding dynamics are effectively replaced by n integrators and a bounded error term. □

6. PRACTICAL EXAMPLES AND SIMULATIONS

Example 1: Consider a system with an input hysteresis whose first order reversal curves are shown on Fig. 3(left) in blue color. Consider modeling this hysteresis with a parametric hysteresis operator (1) and linear input and output shaping functions. Parameters $k_1 = 0.14$, $k_2 = 8$, $\psi_{input}(in(t)) = 0.2 \cdot in(t)$ and $\psi_{output}(out(t)) = 1.4 \cdot out(t)$ where chosen forming an operator $out(t) = 1.4H(0.14, 8)\left[0.2in(t)\right]$ whose reversal curves are shown on Fig. 3(left) in red color. To reproduce the demonstration hysteresis, a family of parametric hysteresis operators $RH(0.14, 0.1, 8, 5)$ would have to be used. Computing the maximal error bound with (15) and (12) gives $\Delta_b \leq 0.13$. This bound is further increased by the output shaping function to $\Delta_b \leq 0.182$. The error is too large, so a different approach is required. Next we try using non-linear shaping functions and the input dependant parameter k_2. The following parameters were obtained: $k_1 = 0.105$, $k_2 = \varphi(in(t)) = 9 - 2 \cdot in(t)$, $\psi_{input}(in(t)) = in(t) - 0.098 \cdot in^2(t)$ and $\psi_{output}(out(t)) = 2.02 \cdot out(t)$. The outcome is shown on Fig. 3(right) where a good match can be observed. The family of parametric hysteresis operators $RH(0.105, 0.005, \varphi(\cdot), 0.5)$ was shown to reproduce all the demonstrated first-order reversal curves. Since an input dependant k_2 was used, results discussed in proposition 4.3 give the additional parameter error: $\Delta k_2{}^* \leq \sup_{in(t)} \frac{d\varphi(in(t))}{din(t)} k_1 = -2 \cdot 0.105 = 0.21$. Values $k_1 = 0.105$, $\Delta k_1 = 0.005$, $\{\min(k_2) = 5, \max(k_2) = 12\}$ and $\Delta k_2 = 1.235$ were used in (15) and (12) to obtain the compensation error bound: $\Delta_b \leq 0.007$ which after applying the output shaping function gives: $\Delta_b \leq 0.014$. Simulation results are shown on Fig. 4.

Example 2: Consider a voltage controlled variable reluctance actuator modeled by:

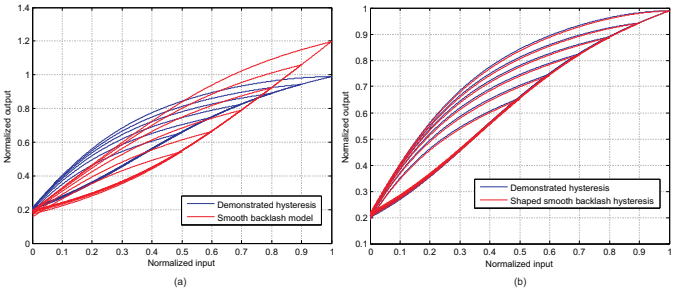

Fig. 3. *Left*: demonstrated hysteresis is not reproducible with a smooth blacklash; *Right*: shaping the smooth backlash gives good results

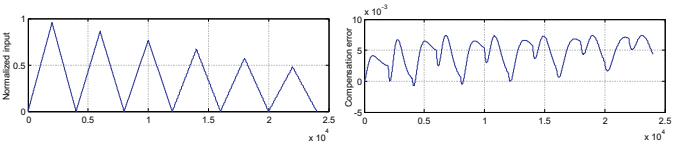

Fig. 4. *Left*: input signal, *Right*: compensation error

$$\dot{I}(t) = -\frac{R}{L} I(t) + \frac{1}{L} U(t)$$
$$\Phi(t) = Hyst(I(t))$$
$$F(t) = K\Phi(t)^2$$

where $R = 1\ \Omega$ and $L = 100\ mH$ are the excitation coil resistance and inductance respectively, Φ is the normalized flux, $Hyst(\cdot)$ is the normalized magnetic hysteresis present in the actuator core and $K = 20$ is some positive constant defining the final force. In this section a feed-forward compensator for the magnetic hysteresis present in the system is designed. To make the hysteresis in the example more realistic, previous measurements of the hysteresis present in a reluctance actuator with a laminated E-shaped Co-Fe alloy magnetic core were used. This data was normalized and the width of the hysteresis loop was increased 30 times to make it clearly visible as shown in Fig. 5(left). A direct parametric hysteresis operator together with a nonlinear *shaping function* is fitted to the data to reproduce first-order reversal curves as accurately as possible. Fitted parameters are: $k_1 = 0.06, k_2 = 5$ and by varying those parameters within bound of $\Delta k_1 = 0.005, \Delta k_2 = 2.5$, the whole curve can be reproduced by a family $RH(k_1, \Delta k_1, k_2, \Delta k_2)$. Bigger values for k_2 give better match closer to zero magnetization, while smaller values give better match closer to saturation. The shaping function: $\psi(v) = v - 0.088v^2 - e^{-(9.6+6.6v)}$ was used to obtain the final hysteresis approximation: $\Phi(t) = \psi\left(H(k_1, k_2)\left[I(t)\right]\right)$. Knowing the robust hysteresis operator family that reproduces the given hysteresis enables the calculation of the error bound of the approximate model using (12) which gives $\Delta_a \leq 0.03$. Inequality (15) then yields the final maximal compensation error bound: $\Delta_b \leq \Delta_a \leq 0.03$. Lemma 5.1 is then applied to obtain the compensation law: $u(t) = L \cdot \dot{H}^{-1}(k_1, k_2)\left[v(t), \dot{v}(t)\right] + R \cdot H^{-1}(k_1, k_2)\left[v(t)\right]$ where $\dot{v}(t) = u_{new}(t)$, which will transform the system to an integrator with an added error Δ_b in series with the remaining non-linearity $(\psi(\cdot))^2$. Simulation results for the proposed compensation scheme are shown in Fig. 5(right) where the compensation error is kept under the calculated bound of $\Delta_b \leq 0.03$. The final maximal force error is 3 N out of maximal 300 N, which is due to

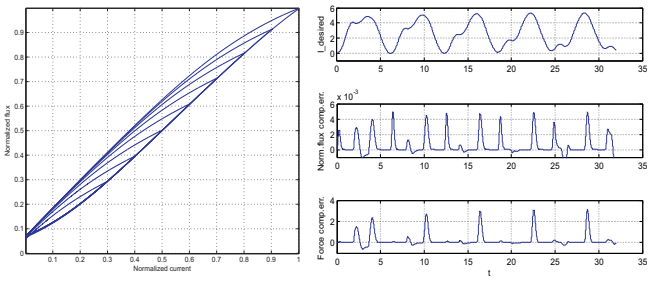

Fig. 5. *Left*: typical shape of a measured normalized hysteresis loop of a Co-Fe alloy; *Right*: compensation error of the proposed hysteresis compensator

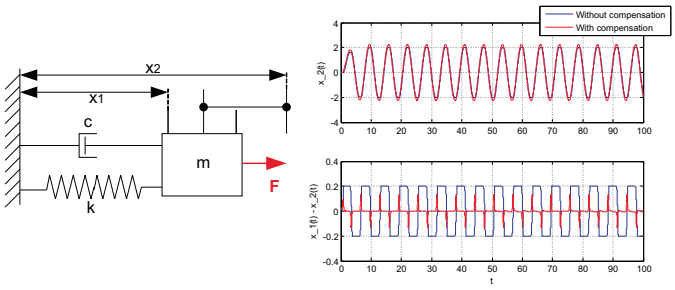

Fig. 6. *Left*: demonstration mechanical system; *Right*: simulation results and the compensation error

the large motor constant $K = 20$ and a quadratic relation between the flux and the force.

Example 3: Consider a simple mechanical system shown in Fig. 6(left). The task is to control the position x_2 using the force F as the input. Mechanical clearance between x_1 and x_2 is described by a non-smooth *backlash* very often seen in mechanical systems. The system model is:

$$m\ddot{x}_1(t) = F(t) - c\dot{x}_1(t) - kx_1(t)$$
$$x_2 = Backlash(x_1)$$

In order to reproduce non-smooth backlash behavior, the parameter k_2 of the smooth hysteretic operator would have to be infinitely large. Regardless, it will be approximated by a finite k_2. Further, it is seen that the system hysteresis is preceded by linear dynamics, meaning the results from lemma 5.1 can be used. Using demonstration parameters: $m = 1$, $k = 1$, $c = 0.9$, BacklashWidth $= 0.4$ and approximating the non-smooth backlash hysteresis with $x_2(t) = H(0.2, 8)\,[x_1(t)]$, the following compensator is obtained by lemma 5.1: $F(t) = \ddot{H}^{-1}(0.2, 8)\,[\ddot{v}(t), \dot{v}(t), v(t)] + 0.9\dot{H}^{-1}(0.2, 8)\,[\dot{v}(t), v(t)] + H^{-1}(0.2, 8)\,[v(t)]$ with $\ddot{v}(t) = -0.9\dot{v}(t) - v(t)$. This control law compensates for the hysteresis, while keeping the same second-order dynamics in open-loop. Simulation results for a periodic input are shown on Fig. 6(right). Very good compensation regardless the approximate nature of the model can be observed. Also, to ideally compensate for mechanical clearance, an infinite control signal would be needed, thus making it impossible in practice. The proposed smooth hysteretic operator gives a good feasible alternative.

7. CONCLUSIONS

This article introduced the smooth backlash behavior as a fundamental property of many hysteretic systems, e.g. ferromagnetic hysteresis and piezoelectric hysteresis. This behavior was modeled in an operator form parameterized by two parameters: the width of the hysteresis and the smoothness of the reversal curves. It was shown that this operator can be easily inverted and shaped using different techniques such as shaping functions and varying parameters to match the desired hysteresis profile. The advantage of having such an operator is that it can be analyzed separately of other effects in the system and the results can be extended to general approaches in the control of systems with hysteresis. One of these approaches is an approximative feed-forward hysteresis compensation based on a parametric hysteresis inverse that was presented in this paper. The main motivation for the future work is to extend the framework based on the operator with new results on algebraic manipulation and harmonic analysis. Simulation results illustrate the analysis.

REFERENCES

D. Angeli, "Systems with counterclockwise input-output dynamics," IEEE Transactions on Automatic Control, vol. 51, no. 7, July, 2006.

G. Bertotti, and I. Mayergoyz, "The science of hysteresis," Academic Press, Feb. 14, 2006.

B.D. Coleman, and M.L. Hodgdon, "A constitutive relation for rate-independent hysteresis in ferromagnetically soft materials," Int. J. Enging. Sci., vol. 24, no. 6, 1986.

R. M. Corless, G. H. Gonnet, D. E. G. Hare, D. J. Jeffrey, and D. E. Knuth. *On the Lambert W function.* Advances in Computational Mathematics, vol. 5, no. 1, 1996.

J.A. Ewing, "Magnetic induction in iron and other metals," London, E.C.: Electrician Printing and Publishing Co., Ltd., 1894.

F. Ikhouane, V. Manosa, and J. Rodellar, "Dynamic properties of the hysteretic Bouc-Wen model," System & Control Letters, vol. 56, no. 3, March 2007.

R.V. Iyer, and X. Tan."Control of hysteretic systems trough inverse compensation," IEEE Control Syst. Mag., vol. 29, no. 1, Feb. 2009.

B. Jayawardhana, H. Logemann, and E.P. Ryan, "PID control of second-order systems with hysteresis," International Journal of Control vol. 81, no. 8, Aug. 2008.

S. Mittal, and C.H. Menq, "Hysteresis compensation in electromagnetic actuators trough Preisach model inversion," IEEE/ASME Transactions on Mechatronics, vol. 5, no. 4, Dec. 2000.

J. Oh, and D.S. Bernstein, "Semilinear Duhem model for rate-independent and rate-dependent hysteresis," IEEE Transactions on Automatic Control, vol. 50, no. 5, May 2005.

J. Oh, B. Drincic, and D.S. Bernstein, "Nonlinear feedback models of hysteresis," IEEE Control Syst. Mag., vol. 29, no. 1, Feb. 2009.

G. Song, J. Zhao, X. Zhou, and J.A. De Abreu-Garcia, "Tracking control of a piezoceramic actuator with hysteresis compensation using inverse Preisach model," IEEE/ASME Transactions on Mechatronics, vol. 10, no. 2, April 2005.

C.Y. Su, Y. Stepanenko, J. Svoboda, and T.P. Leung, "Robust adaptive control of a class of nonlinear systems with unknown backlash-like hysteresis," IEEE Transactions on Automatic Control, vol. 45, no. 12, Dec. 12, 2000.

C.Y. Su, Y. Feng, H. Hong, and X. Chen, "Adaptive control of systems involving complex hysteretic nonlinearities: a generalized Prandtl-Ishlinskii modeling approach," International Journal of Control vol. 82, no. 10, Oct. 2009.

A. Taware, and G. Tao, "Control of sandwich nonlinear systems," Lecture Notes in Control and Information Sciences, Springer-Verlag Berlin Heidelberg, 2003.

G. Tao, and P.V. Kokotovic, "Adaptive control of systems with actuator and sensor nonlinearities," John Wiley & Sons, Inc., New York, 1996.